• Clinical Research •

Retinal microvascular and microstructural alterations in the diagnosis of meibomian gland dysfunction in severely obese population: a new approach

Hai Huang[1], Xiao-Yu Wang[2,3], Hong Wei[4,5], Min Kang[4,5], Jie Zou[4,5], Qian Ling[4,5], San-Hua Xu[4,5], Hui Huang[4,5], Xu Chen[6], Yi-Xin Wang[7], Yi Shao[4,5], Yao Yu[2]

[1]Nanchang Aier Eye Hospital, Nanchang 330006, Jiangxi Province, China
[2]Department of Endocrinology and Metabolism, the First Affiliated Hospital of Nanchang University, Jiangxi Clinical Research Center for Endocrine and Metabolic Disease, Jiangxi Branch of National Clinical Research Center for Metabolic Disease, Nanchang 330006, Jiangxi Province, China
[3]The First Clinical Medical College, Nanchang University, Nanchang 330006, Jiangxi Province, China
[4]Department of Ophthalmology, Eye & ENT Hospital of Fudan University, Shanghai 200433, China
[5]Department of Ophthalmology, the First Affiliated Hospital of Nanchang University, Jiangxi Branch of National Clinical Research Center for Ocular Disease, Nanchang 330006, Jiangxi Province, China
[6]Department of Ophthalmology and Visual Sciences, Maastricht University, Maastricht 6200MA, Limburg Province, Netherlands
[7]School of Optometry and Vision Sciences, Cardiff University, Cardiff CF244HQ, United Kingdom
Co-first authors: Hai Huang and Xiao-Yu Wang
Correspondence to: Yao Yu. Department of Endocrinology and Metabolism, the First Affiliated Hospital of Nanchang University, Nanchang 330006, Jiangxi Province, China. 375135747@qq.com; Yi Shao. Department of Ophthalmology, Eye & ENT Hospital of Fudan University, Shanghai 200433, China. freebee99@163.com
Received: 2023-05-27 Accepted: 2023-11-01

Abstract

● **AIM:** To study retinal microvascular and microstructural alterations in meibomian gland dysfunction (MGD) in severely obese population using optical coherence tomography angiography (OCTA).

● **METHODS:** Twelve MGD patients with severely obese population (PAT group; 24 eyes) and 12 healthy controls (HC group; 24 eyes) were recruited. OCTA images were segmented into five [superior (S), nasal (N), inferior (I), temporal (T), and central foveal (C)] or nine [inner superior (IS), outer superior (OS), inner nasal (IN), outer nasal (ON), inner inferior (II), outer inferior (OI), inner temporal (IT), outer temporal (OT), and C] subregions. The superficial vessel density (SVD), retinal thickness (RT), foveal avascular zone (FAZ) parameters, and retinal volume were measured.

● **RESULTS:** Visual acuity was significantly different between two groups (0.8±0.17 in PAT group *vs* 0.2±0.06 in HC group). SVD was significantly lower in PATs in N, T, OS, IN, OT, and ON. The area under the receiver operating characteristic curve (AUC) for T was 0.961 [95% confidence interval (CI): 0.908 to 1.000], for OS was 0.962 (95%CI: 0.915 to 1.000). RT was significantly lower in PATs in IS, OS, OI, OT, ON, IT, IN, and II. AUC for OT was 0.935 (95%CI: 0.870 to 0.999), for IS was 0.915 (95% CI: 0.838 to 0.992). Angiography results showed significantly lower area and perimeter of FAZ, SVD of the inner retina and both retinal volume and the average volume thickness in the PAT group.

● **CONCLUSION:** Vision may be affected in patients with MGD due to changes in retinal microvessels and microstructures. These changes detected by OCTA may be a potential marker for diagnosing MGD in severe obesity.

● **KEYWORDS:** superficial vessel density; retinal thickness; severely obesity; meibomian gland dysfunction; optical coherence tomography angiography

DOI:10.18240/ijo.2023.12.09

Citation: Huang H, Wang XY, Wei H, Kang M, Zou J, Ling Q, Xu SH, Huang H, Chen X, Wang YX, Shao Y, Yu Y. Retinal microvascular and microstructural alterations in the diagnosis of meibomian gland dysfunction in severely obese population: a new approach. *Int J Ophthalmol* 2023;16(12):1977-1985

INTRODUCTION

Obesity is a serious health risk[1]. Body mass index (BMI) is an indicator used to evaluate obesity. BMI is calculated by dividing weight (kg) by height squared (m^2), with values <25 indicating low weight or regular weight,

25-30 overweight, 30-35 moderate obesity and ≥35 severe obesity[2].

There is growing evidence that obesity is strongly related to metabolic diseases such as diabetes, dyslipidemia and hyperuricemia[3]. Dyslipidemia is also thought to initiate the development of meibomian gland dysfunction (MGD), leading to dry eye and loss of ocular surface homeostasis[4-5].

The meibomian gland is a modified sebaceous gland in cutaneous eyelid that generates meibum, the lipid component of tears[6]. On blinking, meibum is distributed evenly across the ocular surface, protecting the water layer from evaporating and stabilizing the tear film[7]. Any meibomian gland lesions will affect the formation of meibum, thus destabilizing the tear film, and ultimately affecting the corneal steady state, inducing epithelial disruption. As a result, most MGD patients have ocular irritation, such as eye pain and discomfort, and they may also experience symptoms of inflammation[8].

Optical coherence tomography angiography (OCTA) is a significant advance in ocular imaging, producing blood flow images of all retinal vascular layers with unprecedented resolution. OCTA is quick and non-invasive and can offer volumetric data. It allows localization and identification of pathology while providing information about structure and blood flow. OCTA can also be repeated in a single imaging process to obtain comprehensive, extensive microvascular information, or to assess the microvascular response to functional stimuli. In comparison with fluorescein angiography or indocyanine green angiography, OCTA images are not masked by high fluorescence due to dye leakage, so OCTA produces high-contrast, clear microvascular images. Since OCTA does not require an exogenous contrast agent, it can be performed in any patient, especially if fluorescein angiography or indocyanine green angiography are not possible. Finally, OCTA can be executed faster than these other methods, simplifying clinical workflow[9]. It is currently limited, however, by a comparatively small visual field, inability to identify leaks, and image artifacts due to patient movement or blinks[10].

OCTA has provided many important clinical findings, including areas of macular telangiectasia[11], microvascular impairment[12], microaneurysms[13], capillary remodeling[14], and neovascularization[15]. More importantly, OCTA provides unprecedented depth imaging information. It has been applied in assessing many kinds of diseases, including diabetic retinopathy[16], retinal vein obstruction[17], uveitis[18], and glaucoma[19]. It has also been used in neurological research[20] and retinal diagnostics[21]. Therefore, in the present research, we used this technology to evaluate retinal microvasculature and microstructure in MGD patients in severely obese population.

SUBJECTS AND METHODS

Ethical Approval The study methods and protocols were approved by the Medical Ethics Committee of the First Affiliated Hospital of Nanchang University (Nanchang, China; No.2021039) and followed the principles of the Declaration of Helsinki. All subjects were notified of the objectives and content of the study and latent risks, and then provided written informed consent to participate.

Participants Twelve MGD patients in severely obese population (PAT group; 4 females and 8 males) were selected from the Department of Ophthalmology, the First Affiliated Hospital of Nanchang University. Recruitment criteria: 1) BMI≥30; 2) waist circumference ≥85 cm in female, waist circumference ≥90 cm in male; 3) diagnosed as MGD. There are symptoms of dry eye: dryness, foreign body sensation, signs of dry eye: narrowing or interruption of the tear river, and evidence of meibomian gland abnormalities: such as absent meibomian glands, abnormal meibomian gland openings, or abnormal meibomian gland secretions[22]; 4) able to perform OCTA.

This study recruited 12 healthy controls (HC group; 6 females and 6 males), all matched for age and gender in the PAT group. Recruitment criteria: 1) 20≤BMI≤24; 2) able to perform OCTA.

Exclusion criteria: patients in both groups were required to have no 1) mental illness, 2) drug or alcohol abuse history, 3) current pregnancy, 4) history of diseases that lead to OCTA changes: macular hole, cystic macular edema, diabetic retinopathy, age-related macular degeneration, glaucoma, hypertension, diabetes, cerebrovascular disease, Alzheimer's disease, and some intracranial pathologies.

Methods TVue Avanti XR OCTA system (Optovue, Fremont, CA, USA) was used to image both microvascular and retinal cross sections. Scan parameters were scanning rate 70 000 A-scans per second, horizontal definition 22 μm, axial resolution 5 mm, center fold wavelength 840 nm, and bandwidth 45 nm. B-scans were conducted in 3×3 and 6×6 mm^2 scanning modes, five repeated images each at 216 grating positions, were focused on the central fovea, and took 3.9 seconds to complete. A 1080 B-scan (216×five positions) was acquired at 270 frames per second[23]. We used two horizontal and two vertical gratings to obtain 3×3 and 6×6 mm^2 OCTA images through a series of four individual scans. OCTA images of 3-dimensional 3×3 and 6×6 mm^2 en-face were recorded from both eyes.

After scanning, each retinal image was divided into five [superior (S), nasal (N), inferior (I), temporal (T), and central foveal (C)] or nine [inner superior (IS), outer superior (OS), inner nasal (IN), outer nasal (ON), inner inferior (II), outer inferior (OI), inner temporal (IT), outer temporal (OT), and

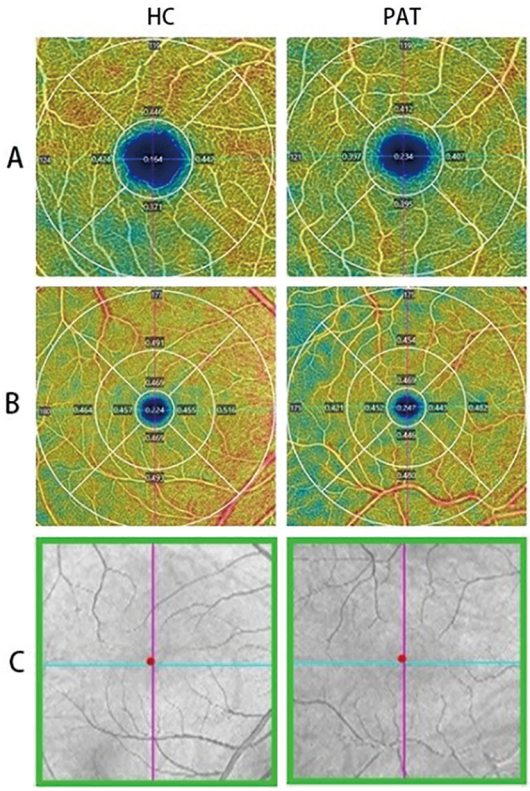

Figure 1 OCTA images of SVD in HC and PAT groups A: 3×3 mm^2 angiography image of superficial vessel; B: 6×6 mm^2 angiography image of superficial vessel; C: OCT fundus. OCTA: Optical coherence tomography angiography; SVD: Superficial vessel density; HC: Healthy control; PAT: Meibomian gland dysfunction patients in severely obese population.

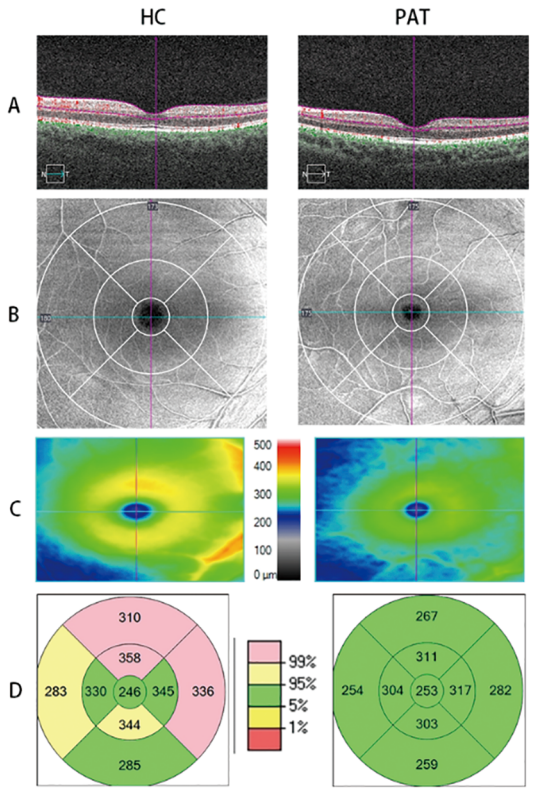

Figure 2 OCTA images and analysis of RT in HC and PAT groups A: Cross-sectional view of RT in the HC and PAT group under OCTA; B: The microstructure of retina in the HC and PAT group under OCTA; C, D: The results of RT in the HC group and PAT group were compared. OCTA: Optical coherence tomography angiography; RT: Retinal thickness; HC: Healthy control; PAT: Meibomian gland dysfunction patients in severely obese population.

C] subregions[24], consisting of two or three concentric circles, and their microvessels and microstructure were investigated. Each retinal layer covered (I) the inner retina (from the inner boundary membrane to the inner plexiform layer), and (II) the whole retina (from the inner boundary membrane to the retinal pigment epithelium). A two-dimensional panoramic image of the superficial retina (between vitreoretinal interface and anterior boundaries of ganglion cell layer) was formed using a threshold method to determine vascular density. According to the pixel size, we scaled the skeleton plate average of the region of interest to calculate the superficial vessel density (SVD) from the fovea to the 3×3 and 6×6 mm^2 brightness gradient image edges. SVD and retinal thickness (RT) were measured and compared. SVD images of each participant were divided into five and nine subregions, and RT images were divided into nine subregions (Figures 1 and 2).

Statistical Analysis SPSS (version 26.0) and GraphPad Prism (version 8.0) were used to analyze data, which were recorded in the form of mean±standard deviation (SD). Independent samples *t*-tests were utilized to analyze data between PAT and HC groups. The relationship between visual acuity and related factors was studied by univariate and multivariate regression analyses. To examine the difference between HC and PAT groups, receiver operating characteristic curves (ROC) were plotted for SVD, RT, FAZ, and retinal volume. $P<0.05$ was considered statistically significant.

Table 1 Characteristics of PATs and HCs mean±SD

Characteristics	PAT group	HC group	*P*
Age (y)	34.27±7.39	31.67±6.24	0.365
Gender (female/male)	4/8	6/6	NA
Weight (kg)	111.92±13.92	66.08±10.88	<0.0001
Visual acuity (logMAR), left	0.80±0.17	0.22±0.06	<0.0001
Visual acuity (logMAR), right	0.83±0.23	0.21±0.08	<0.0001
Systolic blood pressure (mm Hg)	126.67±11.85	130.50±10.83	0.417
Diastolic blood pressure (mm Hg)	82.42±7.67	76.17±10.57	0.112

PAT: Meibomian gland dysfunction patients in severely obese population; HC: Healthy controls; SD: Standard deviation; NA: Not applicable; logMAR: Logarithm of the minimum angle of resolution.

RESULTS

Each group included 12 participants (24 eyes). The groups were statistically matched in age and gender. Visual acuity in PATs was significantly poorer than in HCs ($P<0.0001$; Table 1).

Analysis of the Retinal Superficial Vessel Density SVD of each group is shown in Table 2, Figure 3A, 3B. SVD of PATs

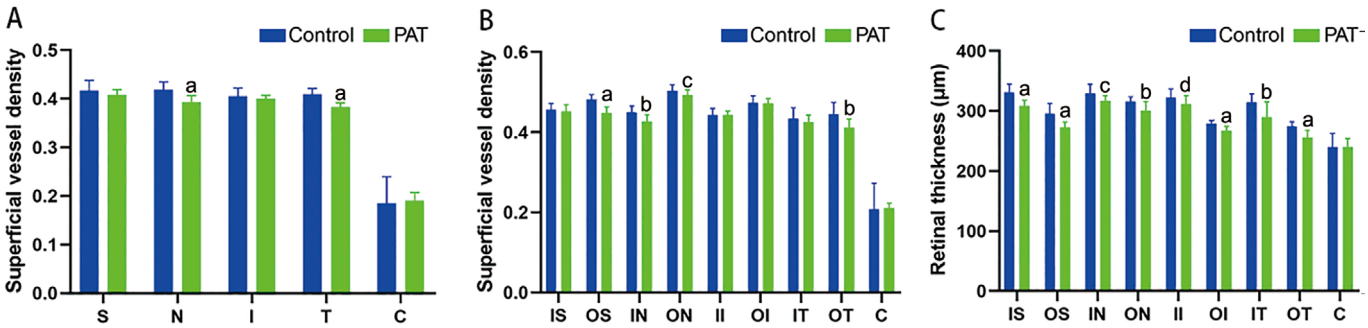

Figure 3 Analysis of SVD and RT results in the PAT group and control group A, B: Analysis of SVD results in the PAT group and control group. The vertical coordinate is the value of SVD, and the horizontal coordinate is the retinal subregions. C: Analysis of RT results in the PAT group and control group. The vertical coordinate is the value of RT, and the horizontal coordinate is the retinal subregions. PAT: Meibomian gland dysfunction patients in severely obese population; SVD: Superficial vessel density; RT: Retinal thickness; S: Superior; N: Nasal; I: Inferior; T: Temporal; C: Central foveal; IS: Inner superior; OS: Outer superior; IN: Inner nasal; ON: Outer nasal; II: Inner inferior; OI: Outer inferior; IT: Inner temporal; OT: Outer temporal. [a]P<0.0001, [b]P<0.001, [c]P<0.01, [d]P<0.01. Bars: Standard errors.

Table 2 Comparison of SVD at different locations between PATs and HCs mean±SD, %

Location	PAT group	HC group	P
S	0.41±0.01	0.42±0.02	0.080
N	0.39±0.01	0.42±0.02	<0.0001
I	0.40±0.01	0.41±0.01	0.185
T	0.38±0.01	0.41±0.01	<0.0001
C	0.19±0.02	0.18±0.06	0.672
IS	0.45±0.02	0.46±0.02	0.217
OS	0.45±0.02	0.48±0.01	<0.0001
IN	0.43±0.02	0.45±0.02	<0.0001
ON	0.49±0.01	0.50±0.02	0.007
II	0.44±0.01	0.44±0.02	0.960
OI	0.47±0.01	0.47±0.02	0.729
IT	0.43±0.02	0.43±0.03	0.195
OT	0.41±0.02	0.44±0.03	<0.0001
C	0.21±0.01	0.21±0.06	0.895

SVD: Superficial vessel density; PAT: Meibomian gland dysfunction patients in severely obese population; HC: Healthy controls; SD: Standard deviation; S: Superior; N: Nasal; I: Inferior; T: Temporal; C: Central foveal; IS: Inner superior; OS: Outer superior; IN: Inner nasal; ON: Outer nasal; II: Inner inferior; OI: Outer inferior; IT: Inner temporal; OT: Outer temporal.

Table 3 Comparison of RT at different locations between PATs and HCs mean±SD, μm

Location	PAT group	HC group	P
IS	308.04±9.73	330.92±14.07	<0.0001
OS	272.67±8.77	295.67±16.98	<0.0001
IN	316.75±8.86	329.08±15.41	0.001
ON	300.58±15.40	315.58±8.05	0.0001
II	311.79±13.71	322.46±14.10	0.011
OI	266.75±7.67	279.08±5.21	<0.0001
IT	289.33±25.73	314.125±14.23	0.0002
OT	256.33±11.95	274.75±6.99	<0.0001
C	240.21±14.35	240.00±22.72	0.970

RT: Retinal thickness; PAT: Meibomian gland dysfunction patients in severely obese population; HC: Healthy controls; IS: Inner superior; OS: Outer superior; IN: Inner nasal; ON: Outer nasal; II: Inner inferior; OI: Outer inferior; IT: Inner temporal; OT: Outer temporal; C: Central foveal.

in N (P<0.0001) and T (P<0.0001) was significantly lower than that of HCs. S, I and C showed no statistically significant difference between the groups. SVD was significantly decreased in PATs in OS, IN, OT (all P<0.0001), and ON (P=0.0068), while no difference was found in IS, II, OI, IT, or C.

Analysis of the Retinal Thickness RT of each group is shown in Table 3, Figure 3C. Compared with HCs, RT was significantly decreased in PATs in IS, OS, OI, OT, ON (P=0.0001), IT (P=0.0002), IN (P=0.0014), and II (P=0.0108). C showed no statistically significant difference between the groups.

Univariate regression analysis showed that visual acuity was negatively correlated with RT (β=-0.634, P<0.001), SVD (β=-0.486, P<0.001), retinal volume (β=-0.651, P<0.001), average volume thickness (β=-0.597, P<0.001), FAZ perimeter (β=-0.507, P<0.001), and FAZ area (β=-0326, P=0.024), but not for FAZ substantiation, blood pressure, age, or gender. Multivariate regression found a significant positive correlation between visual acuity and FAZ perimeters (β=-1.406, P<0.001; Table 4).

ROC Analysis of Superficial Vessel Density and Retinal Thickness Sensitivity and specificity of SVD and RT as diagnostic indicators were investigated by using ROC (Figure 4). Significant between-group differences were found in SVD in all four quadrants and in the central fovea. The

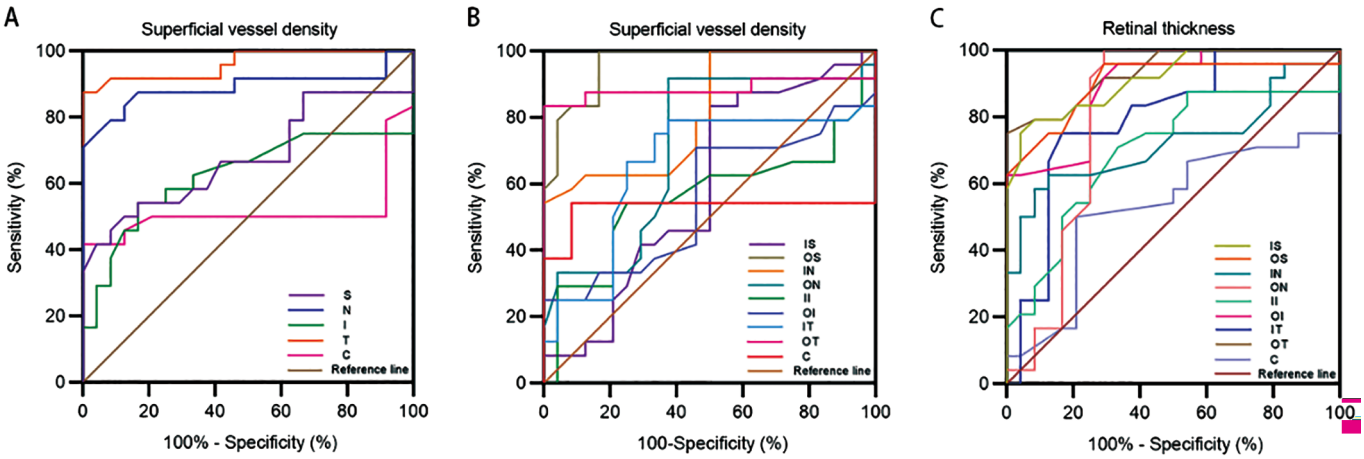

Figure 4 ROC curve analysis of SVD (A, B) and RT (C) ROC: Receiver operating characteristic; RT: Retinal thickness; SVD: Superficial vessel density; S: Superior; N: Nasal; I: Inferior; T: Temporal; C: Central foveal; IS: Inner superior; OS: Outer superior; IN: Inner nasal; ON: Outer nasal; II: Inner inferior; OI: Outer inferior; IT: Inner temporal; OT: Outer temporal.

Table 4 Univariate and multivariate regression analyses of association between visual acuity and related factors

Parameters	Univariate regression analysis				Multivariate regression analysis		
	β	SE	R^2	P	β	SE	P
Age	0.090	0.007	0.008	0.542	-0.002	0.005	0.982
Gender	-0.156	0.099	0.024	0.289	-0.106	0.064	0.272
Systolic blood pressure	-0.077	0.004	0.006	0.604	0.147	0.003	0.150
Diastolic blood pressure	0.237	0.005	0.056	0.105	0.135	0.004	0.224
RT	-0.634	0.003	0.402	<0.001	-0.118	0.004	0.413
SVD	-0.486	3.757	0.236	<0.001	-0.103	3.714	0.422
Volume	-0.651	0.074	0.424	<0.001	-0.204	0.006	0.336
Average volume thickness	-0.597	0.003	0.356	<0.001	-0.204	0.006	0.336
FAZ area	-0.326	0.464	0.107	0.024	1.005	0.940	0.001
FAZ perimeter	-0.507	0.125	0.257	<0.001	-1.406	0.281	<0.001
FAZ substantiation	-0.065	1.188	0.004	0.662	0.231	0.889	0.043

SE: Standard error; RT: Retinal thickness; SVD: Superficial vessel density; FAZ: Foveal avascular zone.

area under the ROC curve (AUC) in the temporal quadrant was 0.961 [95% confidence interval (CI): 0.908 to 1.000], and in the nasal quadrant 0.890 (95%CI: 0.782 to 0.998; Figure 4A), indicating that SVD has a medium to high diagnostic sensitivity in PAT[25]. Significant differences were found between groups in all nine subregions. The AUC in OT was 0.935 (95%CI: 0.870 to 0.999), and 0.915 in IS (95%CI: 0.838 to 0.992), indicating that SVD has a high diagnostic sensitivity for retinal anomalies in PAT (Figure 4B).

Analysis of RT results showed significant differences between groups in all nine subregions. The AUC for OS was 0.962 (95%CI: 0.915 to 1.000), and 0.885 for OT (95%CI: 0.766 to 1.000), indicating medium to high diagnostic sensitivity in PAT (Figure 4C).

Analysis of the Foveal Avascular Zone FAZ analysis in PAT and HC is shown in Table 5 and Figure 5A. In the 3×3 and 6×6 mm^2 angiography results, the area (P=0.0015 and P=0.0039) and perimeter (P=0.0068 and P<0.0001) were significantly decreased in PATs. The AUC was 0.729 for area (95%CI: 0.572 to 0.887), and 0.838 for perimeter (95%CI: 0.704 to 0.972), indicating medium diagnostic sensitivity in PAT.

Analysis of Superficial Vessel Density at Different Retinal Layers The SVDs at different retinal layers in PATs and HCs are shown in Table 5 and Figure 5B. In the 3×3 mm^2 angiography result, the SVD of the retinal inner layer (P<0.0001) was significantly lower in PATs than in HCs, while the central foveal and the full layer showed no difference between groups. In the 6×6 mm^2 angiography result, the SVDs at the retinal inner layer (P<0.0001) and the full layer (P=0.0194) were significantly lower in PATs than HCs. The AUC for 3×3 and 6×6 mm^2 angiography in the retinal inner layer were 0.858 (95%CI: 0.739 to 0.977) and 0.828 (95%CI: 0.712 to 0.944) respectively, indicating medium diagnostic sensitivity in PAT.

Analysis of Retinal Volume and Average Volume Thickness The retinal volume and average volume thickness of the PAT and HC groups are shown in Table 6 and Figure 5C. Compared with HCs, the retinal volume (P=0.0001) and average

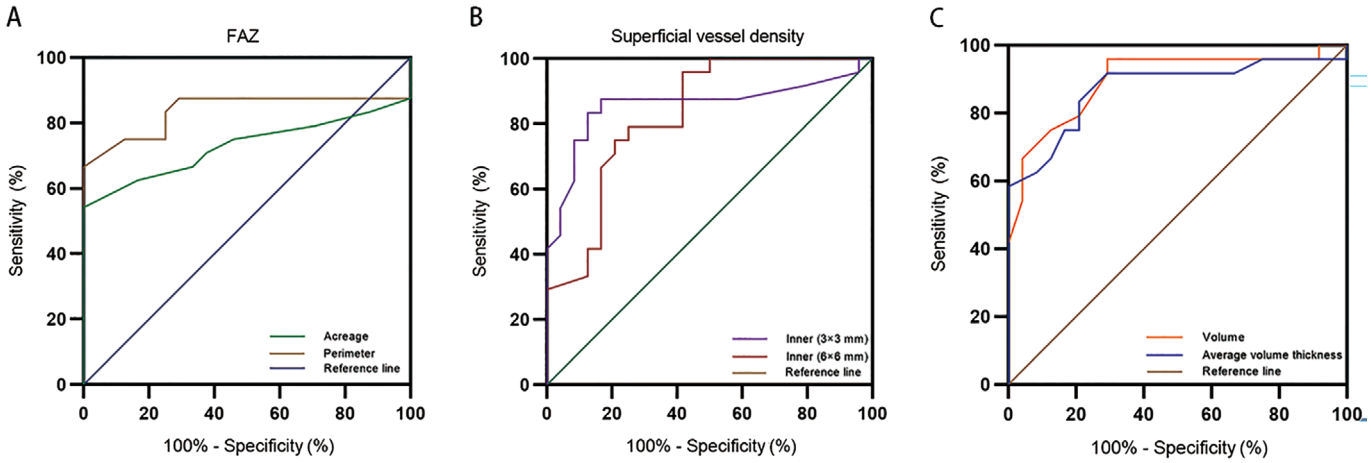

Figure 5 ROC curve analysis of FAZ, inner SVD, and volume A: The area under the ROC curve was 0.729 for area (95%CI: 0.572 to 0.887), and 0.838 for perimeter (95%CI: 0.704 to 0.972); B: The area under the ROC curve was 0.858 for 3×3 mm^2 angiography of inner SVD (95%CI: 0.739 to 0.977), and 0.828 for 6×6 mm^2 angiography of inner SVD (95%CI: 0.712 to 0.944); C: The area under the ROC curve was 0.897 for retinal volume (95%CI: 0.803 to 0.990), and 0.872 for average volume thickness (95%CI: 0.765 to 0.980). ROC: Receiver operating characteristic; FAZ: Foveal avascular zone; SVD: Superficial vessel density.

Table 5 Analysis of FAZ results and SVD results in different retinal layers mean±SD

Parameters	HC group	PAT group	*t*	*P*
Angiography 3×3 mm^2				
FAZ area (mm^2)	0.35±0.13	0.26±0.02	3.386	0.002
FAZ perimeter (mm)	2.37±0.47	2.08±0.13	2.835	0.007
FAZ substantiation	0.74±0.05	0.74±0.06	0.1019	0.919
Central SVD	0.18±0.06	0.19±0.02	0.380	0.706
Inner SVD	0.41±0.01	0.40±0.01	6.096	<0.0001
Full SVD	0.38±0.02	0.38±0.01	0.141	0.889
Angiography 6×6 mm^2				
FAZ area (mm^2)	0.33±0.13	0.25±0.03	3.044	0.004
FAZ perimeter (mm)	2.25±0.39	1.85±0.07	4.842	<0.0001
FAZ substantiation	0.80±0.05	0.79±0.04	0.584	0.562
Central SVD	0.21±0.06	0.21±0.01	0.145	0.885
Inner SVD	0.45±0.02	0.42±0.02	4.926	<0.0001
Outer SVD	0.47±0.01	0.47±0.02	0.215	0.831
Full SVD	0.46±0.01	0.45±0.01	2.424	0.019

FAZ: Foveal avascular zone; SVD: Superficial vessel density; HC: Health control; PAT: Meibomian gland dysfunction patient in severely obese population.

Table 6 Analysis of retinal volume and average volume thickness results mean±SD

Parameters	HC group	PAT group	*t*	*P*
Volume (mm^3)	10.49±0.41	9.80±0.34	6.303	0.0001
Average volume thickness (μm)	289.25±10.43	275.21±7.77	5.288	0.0001

HC: Health control; PAT: Meibomian gland dysfunction patient in severely obese population.

volume thickness (*P*=0.0001) in PATs were both significantly decreased. The AUC for the retinal volume was 0.897 (95%CI: 0.803 to 0.990) and for average volume thickness 0.872 (95%CI: 0.765 to 0.980), indicating moderate to high diagnostic sensitivity in PATs.

DISCUSSION

Our study found significant decrease in visual acuity, retinal SVD, RT, FAZ area and perimeter, retinal volume and average volume thickness in MGD patients in severely obese population than in controls.

MGD is the major causal factor of dry eye and loss of ocular surface homeostasis. More and more research have indicated that dyslipidemia can promote the development of MGD, which is highly associated with severe obesity[26]. Previous studies have shown that moderate to severe MGD is significantly related to high BMI in Chinese adults[27].

The periphery of the retina is a pathological site for several eye diseases. Changes in the retina can provide markers to diagnose and monitor these and to evaluate their therapeutic response. Retinal changes have also been reported in neurodegenerative diseases such as Parkinson's disease[28] and Alzheimer's disease[29]. The retina and the cerebrum develop from the same embryonic tissue, so retinal research may offer a new way to understand systematic diseases that are related to the central nervous system. Since retinal vessels with tight junctions between endothelial cells are similar to cerebrovascular vessels, it is assumed that imaging of the former may be helpful in research on the latter. OCTA has been effectively applied in predicting retinal vascular anomalies in neurological diseases[30]. Schönfeldt-Lecuona *et al*[31] have provided further evidence that in schizophrenia spectrum disorder patients structural changes observed in the brain are also observable in the retina. Retinal research may help to further understand a nervous system that changes in highly complex diseases.

Decreased SVD has been detected in many diseases. OCTA in glaucomatous eyes is characterized by reduced density of superficial blood vessels at the optic disk and in the macular region, and complete loss of choroidal capillaries in localized areas of peripapillary atrophy[19]. Previous research revealed that superficial parapapillary microvascular density is reduced in high myopia[32]. Our study found decreased SVD in MGD patients in severely obese population, and we speculate that those patients may be at risk of the eye diseases mentioned above. Recent research has reported that decreased RT in patients with Alzheimer's disease is correlated with disease severity[33] and outer peripapillary total retinal ring volumes reportedly differentiate papilledema from pseudopapilledema[34]. As these subclinical changes also existed in the PATs group in the present study, we speculate that retinal microvascular and microstructural alterations may facilitate understanding of the pathogenesis of MGD in severely obese population and can be used for early diagnosis and staging of MGD in this population.

Our regression analysis demonstrated that impaired visual acuity was highly correlated with retinal thinning, SVD decrease and FAZ reduction, and a number of previous studies are consistent with these findings. A study on Sjögren's syndrome patients showed that the thinning of the retina affects visual acuity[35] and Islam[36] reported that vision was highly related to RT in diabetic macular edema. Nakajima *et al*[37] found that deep vessel density was highly related to loss of visual field in patients with retinitis pigmentosa. Roesel *et al*[38] reported that foveal thickness was related to vision.

Our ROC curve analysis of SVD, RT, FAZ, and retinal volume illustrates possible approaches for early discovery of retinal variations in MGD patients in severely obese population. Early diagnosis is key to more effective treatment and better prognosis. OCTA and functional magnetic resonance imaging are revolutionary methods for visualization of blood vessels at different layers of the retina and brain[39-42]. Being non-invasive and time-efficient, it has been widely used in retinal diagnostics. Microvascular and microstructural changes in MGD patients in severely obese population may precede clinically distinguishable retinopathy. The SVD, FAZ, RT, and retinal volume detected by OCTA may provide new avenues for the diagnosis of PAT. However, more studies are needed to provide evidence for future application in clinic. Therefore, in view of the important results of our study, more participants need to be enrolled in future research.

Our research has some limitations. The study included a relatively small sample, but despite this, SVD and RT were significantly different between the two groups. These results may contribute to future progress toward more precise methods to test retinal microvascular and microstructural alterations at an early stage. In addition, we found no correlation between SVD and RT in the PATs, which may need to be verified by more large-scale studies in the future.

In conclusion, we used OCTA to detect the retinal microvascular and microstructural alterations in MGD patients in a severely obese population. Our results showed reduced SVD in N, T, OS, IN, ON, OT; thinning of the RT in all subregions except central foveal; reduction in FAZ area and perimeter; significantly reduced SVD in the inner retina; and reduced retinal volume and average volume thickness. In addition, perimeter thinning at the FAZ was found to affect vision. OCTA may provide a new approach for early diagnosis of MGD in severely obese population.

ACKNOWLEDGEMENTS

Foundations: Supported by National Natural Science Foundation of China (No.82160195); Science and Technology Project of Jiangxi Provincial Department of Education (No. GJJ200169); Science and Technology Project of Jiangxi Province Health Commission of Traditional Chinese Medicine (No.2020A0087); Science and Technology Project of Jiangxi Health Commission (No.202130210).

Conflicts of Interest: Huang H, None; **Wang XY,** None; **Wei H,** None; **Kang M,** None; **Zou J,** None; **Ling Q,** None; **Xu SH,** None; **Huang H,** None; **Chen X,** None; **Wang YX,** None; **Shao Y,** None; **Yu Y,** None.

REFERENCES

1 Hales CM, Carroll MD, Fryar CD, Ogden CL. Prevalence of obesity and severe obesity among adults: United States, 2017-2018. *NCHS Data Brief* 2020;(360):1-8.

2 Vivante A, Golan E, Tzur D, Leiba A, Tirosh A, Skorecki K, Calderon-Margalit R. Body mass index in 1.2 million adolescents and risk for end-stage renal disease. *Arch Intern Med* 2012;172(21):1644-1650.

3 Jung UJ, Choi MS. Obesity and its metabolic complications: the role of adipokines and the relationship between obesity, inflammation, insulin resistance, dyslipidemia and nonalcoholic fatty liver disease. *Int J Mol Sci* 2014;15(4):6184-6223.

4 Kuriakose RK, Braich PS. Dyslipidemia and its association with meibomian gland dysfunction: a systematic review. *Int Ophthalmol* 2018;38(4):1809-1816.

5 Osae EA, Steven P, Redfern R, *et al*. Dyslipidemia and meibomian gland dysfunction: utility of lipidomics and experimental prospects with a diet-induced obesity mouse model. *Int J Mol Sci* 2019;20(14):3505.

6 Knop E, Knop N, Millar T, Obata H, Sullivan DA. The international workshop on meibomian gland dysfunction: report of the subcommittee on anatomy, physiology, and pathophysiology of the meibomian gland. *Invest Ophthalmol Vis Sci* 2011;52(4):1938-1978.

7 Nichols KK, Foulks GN, Bron AJ, Glasgow BJ, Dogru M, Tsubota K, Lemp MA, Sullivan DA. The international workshop on meibomian gland dysfunction: executive summary. *Invest Ophthalmol Vis Sci* 2011;52(4):1922-1929.

8 Chhadva P, Goldhardt R, Galor A. Meibomian gland disease: the role of gland dysfunction in dry eye disease. *Ophthalmology* 2017;124(11S): S20-S26.

9 Spaide RF, Fujimoto JG, Waheed NK, Sadda SR, Staurenghi G. Optical coherence tomography angiography. *Prog Retin Eye Res* 2018;64:1-55.

10 de Carlo TE, Romano A, Waheed NK, Duker JS. A review of optical coherence tomography angiography (OCTA). *Int J Retina Vitreous* 2015;1:5.

11 Nakai M, Iwami H, Fukuyama H, Gomi F. Visualization of microaneurysms in macular telangiectasia type 1 on optical coherence tomography angiography before and after photocoagulation. *Graefes Arch Clin Exp Ophthalmol* 2021;259(6):1513-1520.

12 Rommel F, Prangel D, Prasuhn M, Grisanti S, Ranjbar M. Correlation of retinal and choroidal microvascular impairment in systemic sclerosis. *Orphanet J Rare Dis* 2021;16(1):27.

13 Borrelli E, Sacconi R, Brambati M, Bandello F, Querques G. *In vivo* rotational three-dimensional OCTA analysis of microaneurysms in the human diabetic retina. *Sci Rep* 2019;9(1):16789.

14 Arthur E, Alber J, Thompson LI, Sinoff S, Snyder PJ. OCTA reveals remodeling of the peripheral capillary free zones in normal aging. *Sci Rep* 2021;11(1):15593.

15 Mastropasqua R, Evangelista F, Amodei F, D'Aloisio R, Pinto F, Doronzo E, Viggiano P, Porreca A, Di Nicola M, Parravano M, Toto L. Optical coherence tomography angiography in macular neovascularization: a comparison between different OCTA devices. *Transl Vis Sci Technol* 2020;9(11):6.

16 Sun Z, Yang D, Tang Z, Ng DS, Cheung CY. Optical coherence tomography angiography in diabetic retinopathy: an updated review. *Eye(Lond)* 2021;35(1):149-161.

17 Shiraki A, Sakimoto S, Tsuboi K, Wakabayashi T, Hara C, Fukushima Y, Sayanagi K, Nishida K, Sakaguchi H, Nishida K. Evaluation of retinal nonperfusion in branch retinal vein occlusion using wide-field optical coherence tomography angiography. *Acta Ophthalmol* 2019;97(6):e913-e918.

18 Dingerkus VLS, Munk MR, Brinkmann MP, Freiberg FJ, Heussen FMA, Kinzl S, Lortz S, Orgül S, Becker M. Optical coherence tomography angiography (OCTA) as a new diagnostic tool in uveitis. *J Ophthalmic Inflamm Infect* 2019;9(1):10.

19 Rao HL, Pradhan ZS, Suh MH, Moghimi S, Mansouri K, Weinreb RN. Optical coherence tomography angiography in glaucoma. *J Glaucoma* 2020;29(4):312-321.

20 Wang L, Murphy O, Caldito NG, Calabresi PA, Saidha S. Emerging applications of optical coherence tomography angiography (OCTA) in neurological research. *Eye Vis(Lond)* 2018;5:11.

21 Rocholz R, Corvi F, Weichsel J, Schmidt S, Staurenghi G. OCT angiography (OCTA) in retinal diagnostics. In: Bille JF, editor. *High Resolution Imaging in Microscopy and Ophthalmology: New Frontiers in Biomedical Optics* [Internet]. Cham (CH):Springer; 2019. Chapter 6.

22 Kovács B, Láng B, Takácsi-Nagy A, Horváth G, Czakó C, Csorba A, Kiss H, Szalai I, Nagy ZZ, Kovács I. Meibomian gland dysfunction and dry eye: diagnosis and treatment. *Orv Hetil* 2021;162(2):43-51.

23 Kashani AH, Chen CL, Gahm JK, Zheng F, Richter GM, Rosenfeld PJ, Shi Y, Wang RK. Optical coherence tomography angiography: a comprehensive review of current methods and clinical applications. *Prog Retin Eye Res* 2017;60:66-100.

24 Relhan N, Flynn HW Jr. The early treatment diabetic retinopathy study historical review and relevance to today's management of diabetic macular edema. *Curr Opin Ophthalmol* 2017;28(3):205-212.

25 Nahm FS. Receiver operating characteristic curve: overview and practical use for clinicians. *Korean J Anesthesiol* 2022;75(1):25-36.

26 Engin A. Endothelial dysfunction in obesity. *Adv Exp Med Biol* 2017;960:345-379.

27 Mather KJ, Steinberg HO, Baron AD. Insulin resistance in the vasculature. *J Clin Invest* 2013;123(3):1003-1004.

28 Karczewski J, Śledzińska E, Baturo A, Jończyk I, Maleszko A, Samborski P, Begier-Krasińska B, Dobrowolska A. Obesity and inflammation. *Eur Cytokine Netw* 2018;29(3):83-94.

29 Shi H, Koronyo Y, Rentsendorj A, *et al*. Identification of early pericyte loss and vascular amyloidosis in Alzheimer's disease retina. *Acta Neuropathol* 2020;139(5):813-836.

30 Wylęgała A. Principles of OCTA and applications in clinical neurology. *Curr Neurol Neurosci Rep* 2018;18(12):96.

31 Schönfeldt-Lecuona C, Kregel T, Schmidt A, Kassubek J, Dreyhaupt J, Freudenmann RW, Connemann BJ, Gahr M, Pinkhardt EH. Retinal single-layer analysis with optical coherence tomography (OCT) in schizophrenia spectrum disorder. *Schizophr Res* 2020;219:5-12.

32 Guo Y, Sung MS, Park SW. Assessment of superficial retinal microvascular density in healthy myopia. *Int Ophthalmol* 2019;39(8):1861-1870.

33 Kim JI, Kang BH. Decreased retinal thickness in patients with Alzheimer's disease is correlated with disease severity. *PLoS One* 2019;14(11):e0224180.

34 Fard MA, Fakhree S, Abdi P, Hassanpoor N, Subramanian PS. Quantification of peripapillary total retinal volume in pseudopapilledema and mild papilledema using spectral-domain optical coherence tomography. *Am J Ophthalmol* 2014;158(1): 136-143.

35 Liu R, Wang Y, Li Q, Xia Q, Xu T, Han T, Cai S, Luo S, Wu R, Shao Y. Optical coherence tomography angiography biomarkers of retinal thickness and microvascular alterations in Sjogren's syndrome. *Front Neurol* 2022;13:853930.

36 Islam F. Retinal thickness and visual acuity in diabetic macular edema: an optical coherence tomography-based study. *J Coll Physicians Surg Pak* 2016;26(7):598-601.

37 Nakajima K, Inoue T, Maruyama-Inoue M, Yanagi Y, Kadonosono K, Ogawa A, Hashimoto Y, Azuma K, Terao R, Asaoka R, Obata R. Relationship between the vessel density around the optic nerve head and visual field deterioration in eyes with retinitis pigmentosa. *Graefes Arch Clin Exp Ophthalmol* 2022;260(4):1097-1103.

38 Roesel M, Heimes B, Heinz C, Henschel A, Spital G, Heiligenhaus A. Comparison of retinal thickness and fundus-related microperimetry with visual acuity in uveitic macular oedema. *Acta Ophthalmol* 2011;89(6):533-537.

39 Ye L, Zhou SS, Yang WL, *et al*. Retinal microvasculature alteration in active thyroid-associated ophthalmopathy. *Endocr Pract* 2018; 24(7):658-667.

40 Shao Y, Jiang H, Wei Y, *et al*. Visualization of focal thinning of the ganglion cell–inner plexiform layer in patients with mild cognitive impairment and Alzheimer's disease. *J Alzheimers Dis* 2018;64(4):1261-1273.

41 Xu MW, Liu HM, Tan G, *et al*. Altered regional homogeneity in patients with corneal ulcer: a resting-state functional MRI study. *Front Neurosci* 2019;13:743.

42 Wang Y, Shao Y, Shi WQ, *et al*. The predictive potential of altered spontaneous brain activity patterns in diabetic retinopathy and nephropathy. *EPMA J* 2019;10(3):249-259.